ACS APPLIED MATERIALS & INTERFACES

Research Article

www.acsami.org

Supertough Polylactide Materials Prepared through In Situ Reactive Blending with PEG-Based Diacrylate Monomer

Huagao Fang,[†,‡] Feng Jiang,[†] Qianghua Wu,[†] Yunsheng Ding,*[,‡] and Zhigang Wang*[,†]

[†]CAS Key Laboratory of Soft Matter Chemistry, Department of Polymer Science and Engineering, Hefei National Laboratory for Physical Sciences at the Microscale, University of Science and Technology of China, Hefei, Anhui Province 230026, P. R. China

[‡]Provincial Key Laboratory of Advanced Functional Materials and Devices, Institute of Polymer Materials and Chemical Engineering, School of Chemistry and Chemical Engineering, Hefei University of Technology, Hefei, Anhui Province 230009, P. R. China

Supporting Information

ABSTRACT: Supertough biocompatible and biodegradable polylactide materials were fabricated by applying a novel and facile method involving reactive blending of polylactide (PLA) and poly(ethylene glycol) diacylate (PEGDA) monomer with no addition of exogenous radical initiators. Torque analysis and FT-IR spectra confirm that cross-linking reaction of acylate groups occurs in the melt blending process according to the free radical polymerization mechanism. The results from differential scanning calorimetry, phase contrast optical microscopy and transmission electron microscopy indicate that the in situ polymerization of PEGDA leads to a phase separated morphology with cross-linked PEGDA (CPEGDA) as the dispersed particle phase domains and PLA matrix as the continuous phase, which leads to increasing viscosity and elasticity with increasing CPEGDA content and a rheological percolation CPEGDA content of 15 wt %. Mechanical properties of the PLA materials are improved significantly, for example, exhibiting improvements by a factor of 20 in tensile toughness and a factor of 26 in notched Izod impact strength at the optimum CPEGDA content. The improvement of toughness in PLA/CPEGDA blends is ascribed to the jointly contributions of crazing and shear yielding during deformation. The toughening strategy in fabricating supertoughened PLA materials in this work is accomplished using biocompatible PEG-based polymer as the toughening modifier with no toxic radical initiators involved in the processing, which has a potential for biomedical applications.

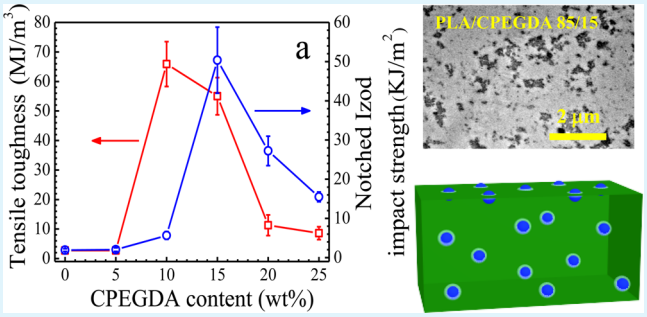

KEYWORDS: *poly(ethylene glycol) diacylate, biodegradable, toughening, phase separation, morphology, mechanical property*

INTRODUCTION

Polylactide (PLA), as a biorenewable, biodegradable, and biocompatible polyester, and derived from the cyclic ester lactide has received great attention in recent years due to the rising environmental protection consideration.[1−3] With mechanical properties similar to polystyrene (PS), PLA is considered to have the highest potential to replace some petroleum-based polymers.[4,5] However, because of the low entanglement density and high value of characteristic ratio, neat PLA exhibits inherent brittleness with values of elongation at break less than 10% and notched impact strength of about 2 kJ/m^2, which has been a major drawback for its large-scale commercial applications.[6−9]

PLA usually deforms in a brittle fashion because of the formation of crazes, and the microcracks bridged by small fibrils and inhomogeneous stress distribution during tensile deformation lead to the catastrophic failure of PLA.[10,11] Various approaches have been adopted to improve the toughness of PLA, including copolymerization,[12−15] and blending with other materials.[10,16−19] Among these approaches, blending is the most economic and effective means. The toughness-modifying materials are usually immiscible with PLA. Therefore, interfacial compatibilizers are added in the blending process to reduce interfacial tension and increase interfacial adhesion. The compatibilizers can be amphiphilic block copolymers containing blocks that are miscible with both the toughness modifiers and PLA. For example, surface modified cellulose nanocrystals were used as a compatibilizer for PLA/nature rubber blends and the elongation at break for the ternary blends increased to 178% at the optimum nature rubber content.[16,17] Chang et al. reported a phase inversion behavior in PLA/soybean oil blends compatibilized by poly(isoprene-*b*-lactide) block copolymers, and the phase morphology was dependent on shear force during blending and block copolymer composition.[18] Poly(ricinoleic acid)-*b*-PLLA diblock copolymer was added in PLA/castor oil blends to control the morphology and improve the tensile toughness.[19]

Reactive blending is a cost-effective technique in situ producing compatibilizers by chemical reactions at the interfaces during melt mixing, which has been widely utilized

Received: May 7, 2014
Accepted: July 28, 2014
Published: August 8, 2014

 © 2014 American Chemical Society

Scheme 1. Chemical Structures of (a) PLA and (b) PEGDA

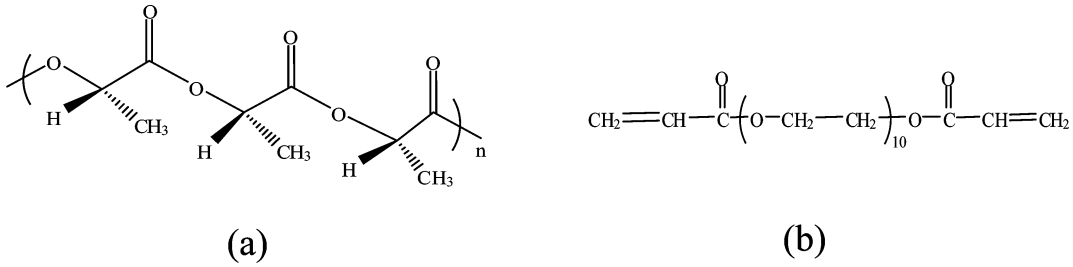

(a) (b)

to improve the toughness of conventional thermoplastic polymers.[20−24] Oyama reported the preparation of supertough PLA blends by reactive blending with poly(ethylene-glycidyl methacrylate) (PEGMA), showing 50-fold increase in impact strength than that of neat PLA.[25] Liu et al. reported the preparation of supertough PLA ternary blends, consisting of PLA, elastomeric ethylene-butyl acylate-glycidyl methacylate terpolymer (EBA-GMA), and zinc ionomer of ethylene-methyacrylic acid copolymer (EMAA-Zn). For this ternary system, dynamic vulcanization in the elastomeric phase and interfacial reactions between epoxy groups of EBA-GMA and the terminal groups of PLA occurred simultaneously at the elevated temperature of 240 °C during the reactive blending process. Effective interfacial compatibilization was thought to be responsible for significant increase in the notched impact strength of PLA materials.[26−29] Bhardwaj and Mohanty reported that hydroxyl functional hyperbranched polymer (HBP) was in situ cross-linked with polyanhydride (PA) in PLA matrix. The prepared blends showed about 570% and 850% improvements in toughness and elongation at break, respectively, which were attributed to the fine dispersion of HBP phase and formation of cross-linked interfaces between HBP phase and PLA matrix.[30]

The recent trend for toughening PLA is to adopt degradable and renewable polymers, including starch,[31,32] poly(ε-caprolactone) (PCL),[33−35] poly(butylene succinate-*co*-adipate) (PBSA),[36,37] polyurethane bioelastomers (PUE),[38] and plant oil derivatives.[39,40] These toughness modifiers are fabricated from renewable resources and are able to degrade completely upon disposal in the environment. Poly(ethylene glycol) (PEG)-based polymers have been widely used in biotechnical and biomedical applications owing to their biocompatibility.[41] PEG can serve as an effective plasticizer for PLA, and the ductility of PLA can be improved by blending with PEG, e.g. high elongation at break and tensile toughness can be achieved. However, a great reduction in the tensile modulus can be a headache at the meanwhile. More unpleasant, the effect of addition of PEG on improvement of the notched impact strength is still poor.[42−44] The crystallization kinetics and crystalline morphology of PLA can be obviously changed by introduction of PEG into PLA.[45−47] There exists a major obstacle for PEG to be utilized as an industrial capable plasticizer for PLA processing, because these binary blends have high tendency to lose mechanical properties with time at ambient temperature due to easy migration of PEG. Sporadic research works have been reported to resolve this problem by increasing molecular mass or introducing cross-linked structure to reduce migration of PEG in PLA matrix. Multifunctional anhydride[48] and isocyanate[49,50] were often used as chain extenders for this purpose. Recently, a method for in situ grafting of PEG on PLA was developed to increase toughness of PLA. PLA was grafted by low molecular mass PEG monoacrylate via reactive blending with dicumyl peroxide (DCP) as a radical initiator. The resulted blends exhibited reduction in the Young's modulus from 1.2 to 0.4 GPa and increase in the elongation at break from 4.7 to 17.9%.[51]

In this work, we designed a novel and facile method for preparation of supertough PLA materials by introduction of in situ cross-linked poly(ethylene glycol) diacylate (CPEGDA) as the rubbery phase. The well dispersed CPEGDA particles were in situ formed in the melt blending process with no addition of any exogenous radical initiators. Fourier transform infrared spectroscopy (FT-IR), differential scanning calorimetry (DSC), rheometer, mechanical property tests, transmission electron microscopy (TEM), and scanning electron microscopy (SEM) were utilized to characterize the chain structures, phase morphologies and mechanical properties and reveal the toughening mechanisms. To the best of our knowledge, such a toughening method for preparation of supertough PLA materials has not been reported elsewhere.

EXPERIMENTAL SECTION

Materials. Commercial available polylactide (PLA) (Natureworks product PLA2002D with L-isomeric content of 96 wt%) was purchased for this study. The PLA sample had a weight-average molecular mass, M_w of 112 kg/mol, polydispersity index of 1.4, and melt flow index of 4.8 g/10 min (190 °C, 2.16 kg). Poly(ethylene glycol) diacrylate monomer (PEGDA, M_n of 575 g/mol) was purchased from Sigma-Aldrich and used as PEG-based diacrylate monomer. Hydroquinone monomethyl ether (MEHQ) of 500 ppm presented as inhibitor in the monomer according to the technical information provided by the supplier. All the chemicals were used as received unless specified. The chemical structures of PLA and PEGDA are illustrated in Scheme 1.

Melt Blending. PLA was dried at 60 °C in a vacuum oven for 12 h before processing. PEGDA was dehydrated by using CaH_2. PLA and PEGDA with mass ratios of 95/5, 90/10, 85/15, 80/20 and 75/25 were mixed in the molten state using an XSS-300 torque rheometer at a rotor speed of 80 rpm. The processing temperature was set at 170 °C. The PLA granules were melted first and then PEGDA was added dropwise. The changes of torque were recorded to evaluate cross-linking reactions of PEGDA during the blending process. For clarification in this study, the binary blends of PLA and in situ produced CPEGDA are coded as PLA/CPEGDA *x*/*y*, where *x* and *y* indicate the mass contents in percentage for PLA and CPEGDA, respectively. For example, PLA/CPEGDA 90/10 stands for PLA/CPEGDA blend with the mass ratio of 90/10. Neat PLA with no addition of PEGDA was prepared by following the same processing procedure for the comparison purpose. To reveal the chemical reactions occurring in the melt blending process, the blend of PLA and PEGDA with the mass ratio of 85/15 was also prepared by solution casting method with chloroform as the common solvent. This blend sample was coded as PLA/PEGDA 85/15. It is noted that the solution casting method was performed at room temperature, which could avoid any thermally induced reactions between PEGDA and PLA.

dx.doi.org/10.1021/am502735q | ACS Appl. Mater. Interfaces 2014, 6, 13552−13563

Chemical Structures. FT-IR spectra of various samples were recorded using a Nicolet Nexus 670 Fourier transform infrared spectroscopy with an attenuated total reflection assembly (FTIR-ATR, Thermo Scientific, MA) to evaluate the chemical reactions in the melt blending process.

Thermal Properties. Thermal properties of the blend samples were measured on a TA Q2000 differential scanning calorimeter (DSC, TA Instruments, New Castle, DE) under a nitrogen flow of 50 mL/min. The samples were taken from the tensile test specimens, aiming to evaluate the effects of crystallinity of the specimens on the mechanical properties. The DSC heat flow curve during the first heating scan at a rate of 10 °C/min was used to examine the initial crystalline state of the PLA matrix phase by determining the cold crystallization temperature (T_{cc}), melting temperature (T_m), enthalpy of cold crystallization (ΔH_{cc}) and enthalpy of melting (ΔH_m). The crystallinity, X_c of PLA was determined using eq 1 as follows:

$$X_c = \frac{\Delta H_m - \Delta H_{cc}}{w_f \Delta H_m^\circ} \times 100\% \quad (1)$$

where w_f is the mass fraction of PLA in the blend, and ΔH_m° is the enthalpy of fusion for the 100% crystalline PLA, taking the value of 93.7 J/g from the literature.[52]

The miscibility between PLA and CPEGDA components was evaluated by the changes of glass transition temperature (T_g) of PLA in the blends. The samples were heated to 200 °C and held for 5 min to erase thermal history and residual stress effects, followed by rapid cooling to −80 °C, and then heated again to 200 °C at a heating rate of 10 °C/min. T_g values were determined from the second heating scan curves.

Rheological Properties. Dynamic rheological measurements on the blend samples were performed on a rotational rheometer (TA-AR2000EX, TA Instruments, New Castle, DE) with a parallel plate geometry of 25 mm in diameter under a nitrogen atmosphere. The gap was set at 0.9 mm. The strain and angular frequency range were 2% and 500−0.1 rad/s, respectively.

Phase Separation Observation by PCOM. To examine the miscibility between PLA and CPEGDA in the melt state, phase contrast optical microscopy (PCOM, Olympus BX51) was applied to observe the phase morphologies for PLA/CPEGDA blends with different mass ratios. The film samples of blends were held at 200 °C for 2 min before the optical micrographs were recorded.

Mechanical Property Tests. The blend samples were compression molded into various specimen forms at 190 °C under vacuum using a homemade vacuum laminator and then quenched to room temperature for mechanical property tests. The tensile properties of the blends were measured at room temperature according to ASTM 638 by using an Instron 3365 universal testing machine (Illinois Tool Works Inc., Norwood, MA). The dumbbell-shaped specimens with thickness of 1 mm, width of 4 mm and length of 80 mm were prepared for the tensile tests. The crosshead speed was set at 10 mm/min. The notched Izod impact strength tests were performed following ISO180 by using a ZBC 1400−1 pendulum impact tester (Shenzhen SANS Test Machine Company, China). The size of the rectangular specimen was 80 × 10 × 3 mm with a 45° V-shaped notch (upper radius of 0.25 mm and depth of 3 mm). The average values from measurements on five specimens were used for data analyses.

Phase Morphological Observations by TEM and SEM. The phase morphologies of the dispersed CPEGDA particles in PLA matrix were further examined by using transmission electron microscopy (TEM, JEOL 2100F) at an accelerated voltage of 200 kV. The ultrathin sections of less than 100 nm in thickness were sliced from the blend samples by using a Leica UC6 cryo-ultramicrotome and subjected to TEM observation directly. For the purpose of particle size analyses, at least 200 particles from independent TEM micrographs were analyzed by using the image processing software (ImageJ, NIH, U.S.A.). It is noted that the particles with sizes too small to be observed at the chosen magnification have been neglected. The cross-sectional area (A_i) of each individual particle (i) was measured and converted into an equivalent diameter of a sphere using eq 2 as follows:

$$d_i = 2\sqrt{A_i/\pi} \quad (2)$$

The number-average particle diameter, d_n, and mass-average particle diameter, d_m, were determined using eqs 3 and 4 as follows:

$$d_n = \frac{\sum n_i d_i}{\sum n_i} \quad (3)$$

$$d_m = \frac{\sum n_i d_i^2}{\sum n_i d_i} \quad (4)$$

where n_i is the number of particles having the particle diameter d_i. The particle size polydispersity was represented as the ratio of mass-average particle diameter, d_m to the number-average particle diameter, d_n, that is, d_m/d_n. The interparticle distance, or matrix ligament thickness (T), was calculated by following the method proposed by Liu,[53] and the detailed description on the calculation can be found in the Supporting Information.

To evaluate the deformation mechanism of the blends, the tensile-fractured surfaces of neat PLA and PLA/CPEGDA 85/15 were sputter-coated with gold and the surface morphologies were examined by a field-emission scanning electron microscopy (SEM, FEI Sirion200, USA).

RESULTS AND DISCUSSION

Thermally Induced Reactions of PEGDA in PLA Matrix. Free radical polymerization of PEG-based diacrylate with different PEG segmental molar masses has been applied to produce cross-linked materials with diverse structures for various application purposes.[54−56] A recent study has revealed that the cross-linking reaction of PEGDA can take place by a simple microwave-induced heating with no addition of any exogenous thermal initiators.[56] In this work, the rheological measurement was applied to examine the thermally induced cross-linking reaction of PEGDA monomer at elevated temperatures without addition of exogenous thermal initiators. Figure 1a shows the change of complex viscosity, $|\eta^*|$ as a function of temperature for PEGDA during a heating process. The rapid increase of complex viscosity at the vicinity of 116 °C indicates that the thermally induced polymerization of diacrylate in PEGDA can take place without addition of exogenous thermal initiators. The polymerization may be initiated by free radical species such as radical impurities, peroxides, and oxygen plasma, resulting in the change of the material state from a viscous liquid into a transparent and brittle solid.

Even though the contents of PEGDA monomer in the blends for the reactive blending process were much lower than that in the bulk polymerization performed on the rheometer, *in situ* polymerization of PEGDA in deed occurred in the PLA matrix, which could be tracked by monitoring the changes of torque during the processing duration (Figure S1 in the Supporting Information). The torque for neat PLA decreases gradually in the melt blending process due to hydrolysis of PLA. However, the torque for the blends continuously increases with time and then levels off at the late stage of the melt blending process, indicating that the cross-linking reaction proceeds gradually and is completed within the blending period of 10 min. Figure 1b shows the change of final torque as a function of the incorporated PEGDA monomer in the blends. The final torque of the blends obviously increases with increasing PEGDA content, reflecting the increasing melt viscosity because of the formation of some new structures in the blending process.

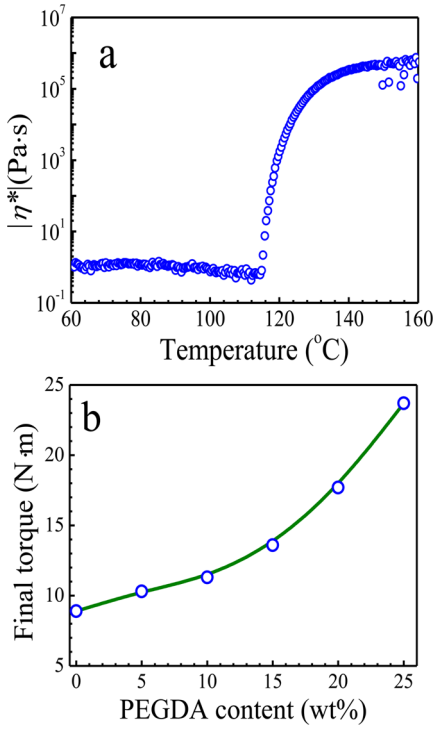

Figure 1. (a) Change of complex viscosity, $|\eta^*|$, as a function of temperature for PEGDA monomer with a temperature ramping rate of 2 °C/min, and (b) change of final torque as a function of PEGDA content for PLA/PEGDA blends in the reactive blending process.

Fourier transform infrared spectroscopy with an attenuated total reflection assembly (FTIR-ATR) was utilized to examine the molecular structural changes in the reactive blending process. Figure 2 shows FTIR-ATR spectra in the range of

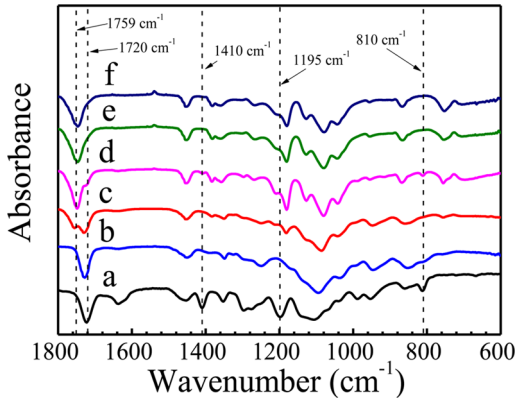

Figure 2. FTIR-ATR spectra for (a) PEGDA monomer, (b) cross-linked PEGDA obtained in the temperature ramping measurement, (c) extracted CPEGDA from PLA/CPEGDA 85/15 as prepared by reactive blending, (d) PLA/PEGDA 85/15 as prepared by solution casting, (e) PLA/CPEGDA 85/15 as prepared by reactive blending, and (f) neat PLA.

1800−600 cm^{-1} for PEGDA monomer, cross-linked PEGDA obtained in the temperature ramping measurement performed on the rheometer, extracted CPEGDA from PLA/CPEGDA 85/15 as prepared by reactive blending, PLA/PEGDA 85/15 as prepared by solution casting, PLA/CPEGDA 85/15 as prepared by reactive blending, and neat PLA, respectively. The spectrum for PEGDA monomer shows absorption bands of acrylic vinyl groups at 810 cm^{-1} (ascribed to the twisting vibration of acrylic CH_2═CH bond), 1410 cm^{-1} (deformation of CH_2═CH bond), and 1198 cm^{-1} (acrylic C═O bond). These characteristic absorption bands of acrylic vinyl groups disappear in the spectra for both the cross-linked PEGDA obtained in the temperature ramping measurement and extracted CPEGDA, indicating that the reactions of acrylic vinyl groups occur with a high conversion due to thermal treatment. The shift of absorption band of carbonyl group from 1720 cm^{-1} (C═O of monomer, curve a) to 1727 cm^{-1} (C═O of polymer, curves b and c) can be also seen in Figure 2. Similarly, the spectrum of PLA/CPEGDA 85/15 as prepared by reactive blending does not show the characteristic absorption bands of acrylic vinyl groups, implying that PEGDA monomers become cross-linked during the thermal treatment. Noticeably, an absorption band at 1759 cm^{-1} is visible for the extracted CPEGDA, which originates from the stretching vibration of ester carbonyl groups in PLA. The appearance of this characteristic absorption band for PLA in the extracted CPEGDA infers that PLA reacts with PEGDA during the melt blending process, keeping in mind that the free PLA homopolymer has been removed by the extraction process (repeated cycles of dissolution, centrifugation and solvent wash). The extracted CPEGDA probably experienced some transesterification reactions between PLA and PEGDA during the melt blending process. Similar interfacial transesterification reactions in reactive blending process have been reported for other PLA/polyester blends.[57,58]

On the basis of the above chemical structure changes, the reaction mechanisms for PEGDA monomer and between cross-linked PEGDA and PLA during the melt blending process can be proposed, which are schematically illustrated in Scheme 2. When PEGDA is added dropwise in PLA melt, the acrylic vinyl groups are initiated and polymerized according to the free radical polymerization mechanism (route a in Scheme 2). The resultant polymer possesses a highly cross-linked structure due to the bifunctional groups in PEGDA monomer (structure I in Scheme 2). Meanwhile, the transesterification between PLA and PEGDA occurs (route b), resulting in grafting of PLA chains on the cross-linked PEGDA (structure II). Some free radicals on moiety of the growing polymer chains are terminated (route c), leading to some dangling PEG chains on cross-linked PEGDA (structure III). This termination reaction causes disappearance of the characteristic vinyl groups in FT-IR spectrum of the extracted CPEGDA. Eventually, the combination of routes a−c leads to structure 4, in which the highly cross-linked PEGDA (CPEGDA) can be grafted with both PEG and PLA chains.

Reaction-Induced Phase Separation. In the reactive blending process, the morphologies of the blends depend on many factors, including the mixing conditions, mass fraction, reaction activities of the functional groups and viscosity ratio of the polymer components. In this study, all the reactive blending processes were performed in a batch mixer with a rotor speed of 80 rpm for 10 min. The in situ formed CPEGDA phase domains (particles) suspend in PLA matrix, leading to different physical appearances of PLA/CPEGDA blend sheets. The blend discs prepared by reactive blending are opaque in appearance and the degree of opacity increases with increasing CPEGDA content, as shown in insets of Figure 3. In contrast, PLA/PEGDA 85/15 sheet prepared via solution casting is quite clear in appearance (Figure S2 in the Supporting Information), indicating sufficient miscibility between PLA and PEGDA

Scheme 2. Illustration of the Reaction Mechanisms for PEGDA Monomer and between Cross-Linked PEGDA and PLA during the Reactive Blending Process

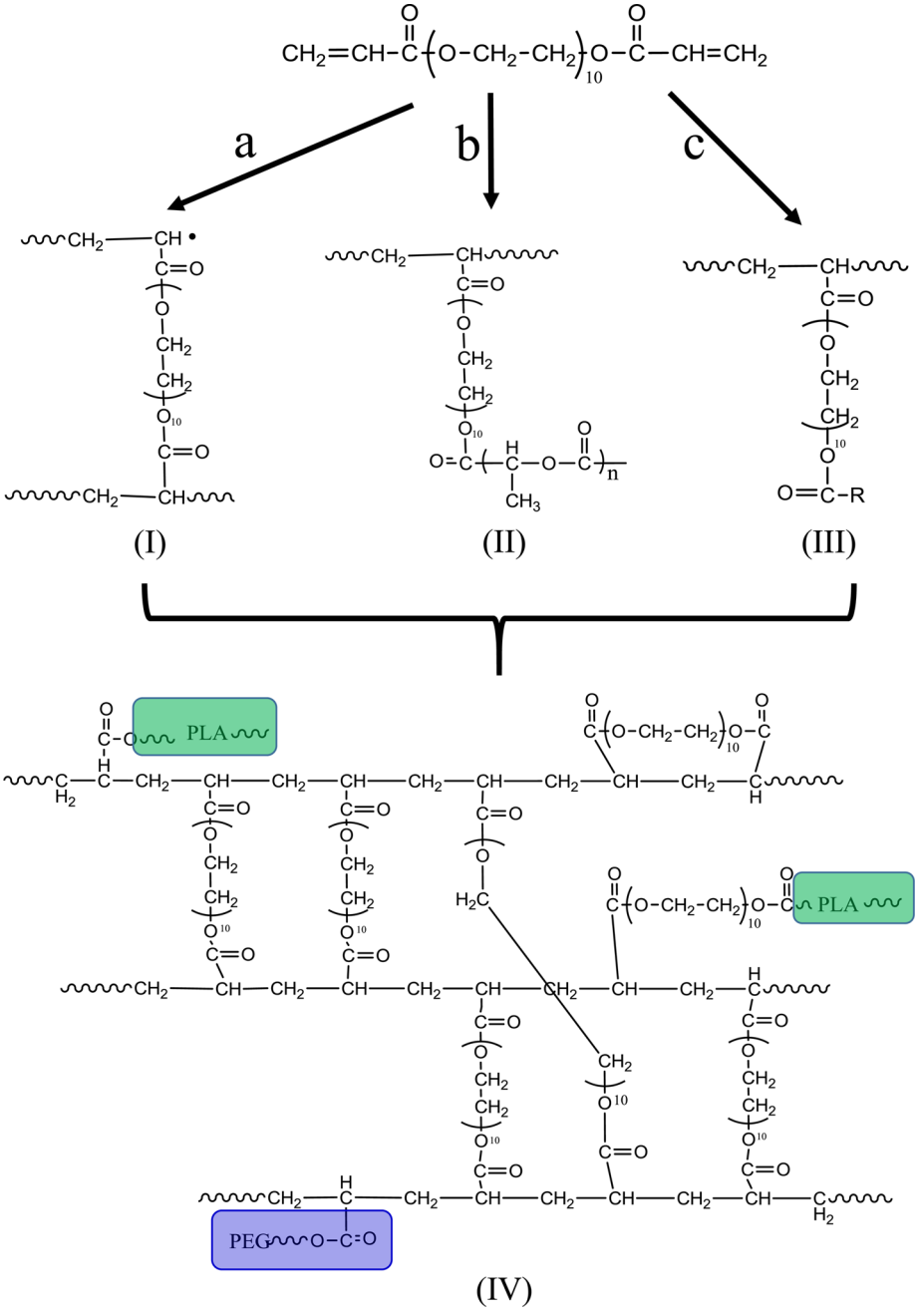

monomer, which is in consistence with the results in the literature.[42−44,46]

The phase separation morphology of PLA/CPEGDA blends can be observed by phase contrast optical microscopy (PCOM). Figure 3 shows the phase contrast optical micrographs for PLA/CPEGDA blends with different mass ratios. Phase separation cannot be observed for PLA/CPEGDA blend with low CPEGDA content (the 95/5 blend) because of small diameters of CPEGDA particles in the molten PLA matrix. With further increasing CPEGDA content, the blends show distinct phase separated morphology, indicating that the in situ formed CPEGDA becomes immiscible with PLA.

The immiscibility between PLA and CPEGDA can be further confirmed in high degree of sensitivity by assessing the change of glass transition temperature, T_g of PLA component in the blends. The Fox equation (eq 5) has been widely applied to predict T_g for miscible binary blend systems.

$$\frac{1}{T_g} = \frac{W_1}{T_{g1}} + \frac{W_2}{T_{g2}} \tag{5}$$

where W_1 and W_2 are mass fractions for polymers 1 and 2 in the blends, respectively. Figure 4 shows DSC heat flow curves during the second heating scans for neat PLA, CPEGDA, and PLA/CPEGDA blends with different mass ratios at a heating rate of 10 °C/min. Note that the second heating scans are adopted in the analysis to minimize the effect of thermal histories. All the blends with different mass ratios exhibit T_g values of PLA component, suggesting that CPEGDA is basically

dx.doi.org/10.1021/am502735q | ACS Appl. Mater. Interfaces 2014, 6, 13552−13563

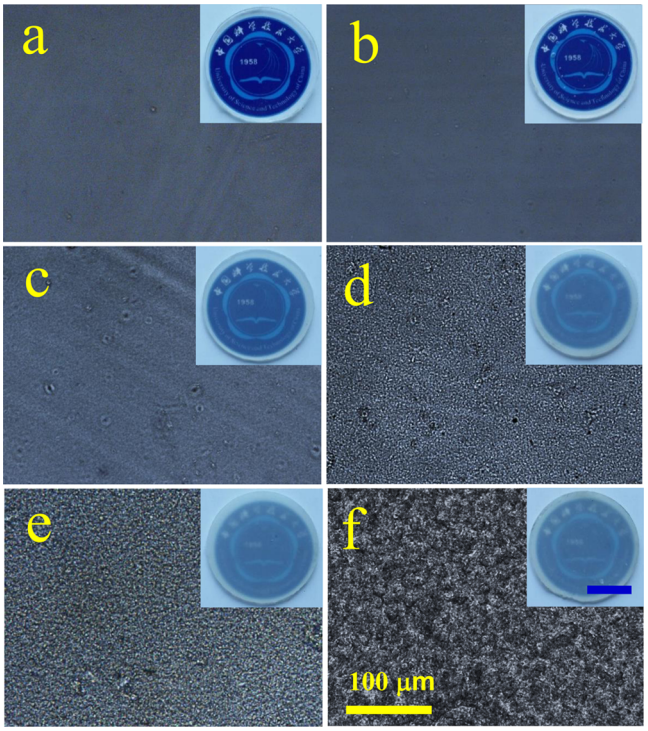

Figure 3. Phase contrast optical micrographs observed at 200 °C for neat PLA (a) and PLA/CPEGDA blends with mass ratios of 95/5 (b), 90/10 (c), 85/15 (d), 80/20 (e), and 75/25 (f). The yellow scale bar in (f) represents 100 μm and is applied to all other micrographs. The insets are photos of the sample discs showing the change of transparence with increasing CPEGDA content. The blue scale bar in inset of panel f represents 10 mm and is applied to all other insets.

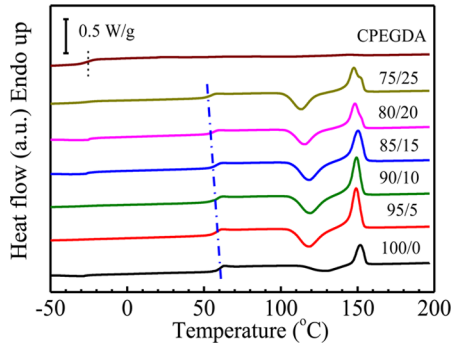

Figure 4. DSC heat flow curves at a heating rate of 10 °C/min for neat PLA, PLA/CPEGDA blends with different mass ratios and CPEGDA extracted from PLA/CPEGDA 85/15. The scale bar represents the heat flow magnitude of 0.5 W/g.

immiscible with PLA. The T_g values of neat PLA and CPEGDA are 61 and −25 °C, respectively. If assuming two components in the blends are miscible, the theoretical T_g values of the blends can be calculated by using the Fox equation according to mass ratios of the two components. However, the observed T_g values for the blends are much higher than that calculated from the Fox equation. For example, the observed T_g values for PLA/CPEGDA 85/15 and 75/25 are 58 and 55 °C, respectively, obviously higher than the calculated T_g values of 42 and 31 °C, respectively. The mismatch reveals that CPEGDA is immiscible with PLA. On the other hand, the blends show slight decreases in T_g with increasing CPEGDA content, for example, the T_g of PLA/CPEGDA 75/25 drops to 55 °C when 25 wt % of CPEGDA is incorporated. The slight decrease in T_g can be attributed to the plasticization effect of CPEGDA in PLA matrix. The dangling chains of PEG acrylate on the surface of CPEGDA particles enhance the plasticization effect with increasing CPEGDA content in PLA matrix. We emphasize here that the reduction of T_g is much more obvious when PLA is plasticized by PEG (Figure S3 in the Supporting Information). Note that PEG with molar mass of 400 g/mol was utilized for the purpose of comparison, which possessed the same number of $-CH_2CH_2O-$ repeat unit as that of PEGDA monomer in this study.

Rheological Behaviors of PLA/CPEGDA Blends. During the reactive blending process, the final torque of the blends increases with increasing PEGDA content, qualitatively reflecting the increasing melt strength as a result of formation of more content of CPEGDA in PLA matrix. Small amplitude oscillatory frequency sweeps were performed at the temperature of 180 °C to examine the effect of incorporated CPEGDA on improvements of melt strength for the blends, such as the complex viscosity, storage modulus, loss modulus, and loss tangent.

The presence of CPEGDA can change the viscosity and degree of shear-thinning as compared with neat PLA. The changes of complex viscosity, $|\eta^*|$, as functions of the applied angular frequency for neat PLA and PLA/CPEGDA blends with different mass ratios are shown in Figure 5. It can be seen

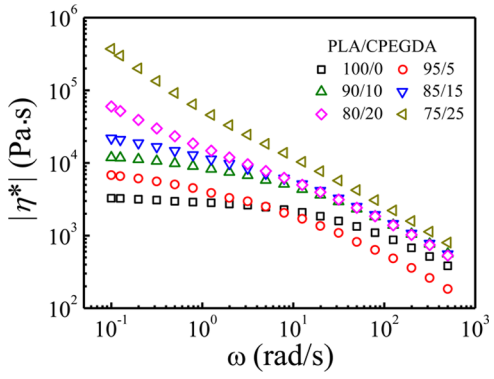

Figure 5. Changes of complex viscosity, $|\eta^*|$, as functions of angular frequency, ω at 180 °C for neat PLA and PLA/CPEGDA blends with different mass ratios.

that the complex viscosity of the blends at the low angular frequencies increases with increasing amount of PEGDA incorporated in the reactive blending process. Two types of frequency dependence of the complex viscosity can be found for the blends. For neat PLA and the blends with low contents of CPEGDA (below 15 wt %), the complex viscosity remains constant over a certain low frequency range and then decreases with further increasing frequency, indicating a transition from the Newtonian plateau to power law regime at the inflection point. For the blends with high contents of CPEGDA (20 and 25 wt %), the Newtonian shear flow behavior is hard to observe in the experimental frequency range as illustrated by the absence of frequency-independent viscosity, indicating that the blends follow more obviously the power law at the low frequencies. The enhancement of shear-thinning for the blends becomes stronger with increasing amount of incorporated CPEGDA. The above phenomenon is related to the phase structures of PLA/CPEGDA blends through in situ formation of CPEGDA particles in PLA matrix. Different from the

plasticization effect of PEG, which reduces the viscosity of PLA, the CPEGDA particles of sufficient amounts in PLA/CPEGDA blends obviously reduce the chain mobility of PLA, resulting in the much enhanced viscosity. Note that for PLA/CPEGDA 95/5 the loosely cross-linked PEGDA containing flexible dangling chains of PEG acrylate can facilitate the chain segmental mobility of PLA in the matrix, leading to reduction of complex viscosity below that of neat PLA at the high angular frequency.

Besides the complex viscosity, the changes of storage modulus and loss modulus with angular frequency of the blends are also sensitive to the CPEGDA content. Figure 6a shows the changes of storage modulus, G', and loss modulus, G'', as functions of angular frequency, ω for neat PLA and PLA/CPEGDA blends with different mass ratios. For linear polymers with narrow molecular mass distribution, G' and G'' in the terminal region follow the well-known frequency dependences, that is, $G' \propto \omega^2$ and $G'' \propto \omega$, for which only the longest relaxation times contribute to the viscoelastic behavior. At the low frequencies, neat PLA sample shows a typical response of a viscous material with the scaling property of approximate $G' \propto \omega^2$ and $G'' \propto \omega$, indicating a liquid-like behavior. With increasing CPEGDA content, the slope of G' at the low frequencies decreases for PLA/CPEGDA blends. For PLA/CPEGDA 85/15, the slope of G' equals to that of G'', indicating a transition from the liquid-like to solid-like behaviors. When the contents of CPEGDA in the blends are 20 and 25 wt %, the values of G' become higher than G'' in the whole frequency range, indicating a typical solid-like behavior.

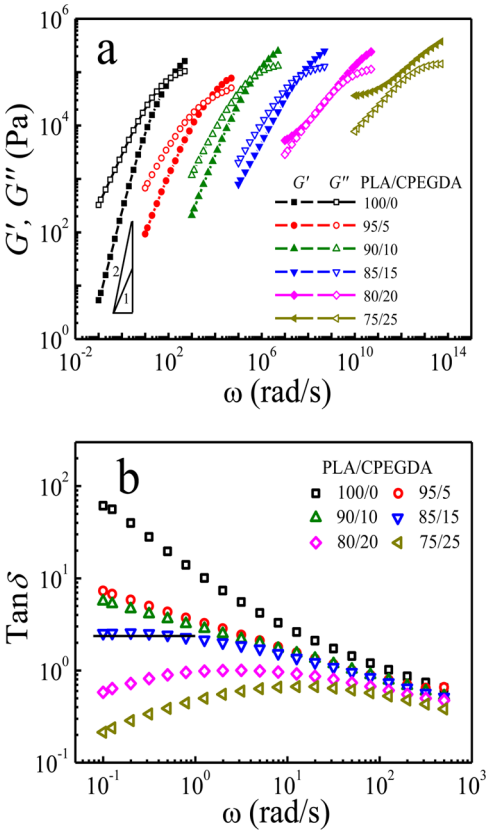

Figure 6. (a) Changes of storage modulus, G' and loss modulus, G'' as functions of angular frequency, ω and (b) frequency dependences of tan δ at 180 °C for neat PLA and PLA/CPEGDA blends with different mass ratios. In panel a, G' and G'' curves are shifted horizontally for providing clear comparison and avoiding overlap of the curves.

Changes in the rheological parameter, loss tangent (tan $\delta = G''/G'$) during the frequency sweeps provide confirmative fingerprints for indicating the formation of cross-linked PEGDA network in PLA matrix. According to Winter and Chambon, the frequency independence of loss tangent can be used to define the gel point for cross-linking systems.[59,60] The method was also widely adopted for polymer composites and blends to estimate the percolation thresholds of the fillers or dispersion phases.[61,62] Figure 6b shows the frequency dependences of tan δ at 180 °C for neat PLA and PLA/CPEGDA blends with different mass ratios. For neat PLA, tan δ is ascending with decreasing angular frequency, which is a typical terminal behavior for a liquid-like material. Behaving differently, PLA/CPEGDA blends demonstrate a gel-like behavior, showing much less significant frequency dependence of tan δ. With increasing CPEGDA content, tan δ of PLA/CPEGDA blends decreases quickly at the low angular frequencies. Tanδ decreases continually and eventually a plateau is reached when incorporating more cross-linked PEGDA into the blends. The frequency independence of tan δ in the low frequency range for PLA/CPEGDA 85/15 reflects a transition from a liquid-like to a gel-like behavior, inferring an appearance of a threshold CPEGDA content for the network formation.

Analysis on Crystallinity of PLA/CPEGDA Blends. PLA is a typical semicrystalline polymer, and its physical, mechanical, and thermal resistance properties are highly dependent on the crystallinity and crystalline morphology in the solid state. Bai et al. reported the methods to tailor impact toughness of PLA/PCL blends by controlling crystallization of PLA matrix and concluded that toughening of the blends became easier to achieve with increasing crystalline content in PLA matrix.[34] However, for the PLA/EBA-GMA/EMAA-Zn ternary blends Liu et al. found that the enhanced crystallization of PLA matrix did not appear to be a contributing factor to the significant dependence of impact toughness on processing temperature.[26] In order to clarify whether PLA crystallization had any influences on the mechanical properties, the thermal properties (crystallization and melting behaviors) were examined for the PLA/CPEGDA blends.

Figure 7 shows the DSC heat flow curves during the first heating scan for neat PLA and PLA/CPEGDA blends. Table 1

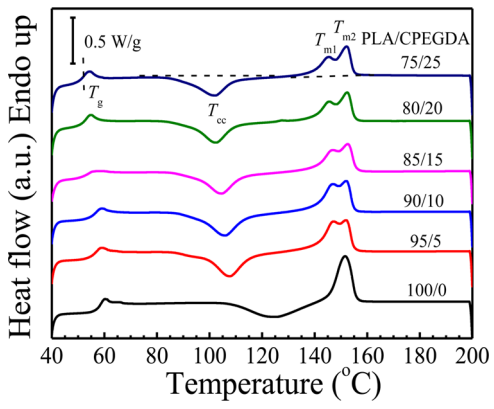

Figure 7. DSC heat flow curves during the first heating scan with a heating rate of 10 °C/min for neat PLA and PLA/CPEGDA blends with different mass ratios. The scale bar represents the heat flow magnitude of 0.5 W/g.

dx.doi.org/10.1021/am502735q | ACS Appl. Mater. Interfaces 2014, 6, 13552−13563

Table 1. Thermal Properties for Neat PLA and PLA/CPEGDA Blends with Different Mass Ratios

sample code	T_{cc} (°C)	T_{m1} (°C)	T_{m2} (°C)	ΔH_c (J/g)	ΔH_m (J/g)	X_c[a] (%)
neat PLA	125		152	19.4	20.1	0.7
PLA/CPEGDA 95/5	108	147	152	23.5	24.3	0.8
PLA/CPEGDA 90/10	106	147	152	25.4	25.8	0.4
PLA/CPEGDA 85/15	104	147	152	24.0	24.4	0.4
PLA/CPEGDA 80/20	102	145	152	23.7	24.4	0.7
PLA/CPEGDA 75/25	102	145	152	24.4	25.1	0.7

[a]The values of crystallinity, X_c are normalized regarding to the mass contents of PLA in the blends.

summarizes the thermal properties obtained from the first heating scan, revealing crystallinities of PLA component in the molded blend samples. As shown in Figure 7, an exothermic peak, attributed to the cold crystallization during heating, is observed for neat PLA and the blends. As compared with neat PLA, the cold crystallization of PLA in the blends occurs at much lower temperatures, T_{cc} and the exothermic peak becomes narrower. The double endothermic melting peaks ranging from 140 to 160 °C are ascribed to the melting of PLA crystals in the blends, with the lower temperature melting peak, T_{m1} relating to melting of less perfect PLA lamellar crystals, and the higher temperature melting peak, T_{m2} to melting of more perfect PLA lamellar crystals. Furthermore, PLA in the blends shows relatively higher values of cold crystallization enthalpy, ΔH_c and the corresponding melting enthalpy, ΔH_m than that in neat PLA. The result suggests that the incorporation of CPEGDA in the blends enhances crystallization of PLA component. The insignificant differences between the values of ΔH_c and ΔH_m for neat PLA and the blends indicate that the initial crystallinities in the blend samples contributing to the mechanical properties are much low (less than 1% in Table 1), which is because of the much slow crystallization rate of PLA in the samples during the quenching process.

Mechanical Properties of PLA/CPEGDA Blends. Figure 8 shows the typical nominal stress−strain curves during tensile deformation for neat PLA and PLA/CPEGDA blends with different mass ratios. The result indicates that the tensile deformation behaviors of the blends display a transition from the brittle to ductile fractures. Neat PLA is a rigid material, which deforms in a brittle fashion. No obvious yield can be observed in its stress−strain curve and the elongation at break is only about 6%, consistent with the results in the literatures.[4,52] PLA/CPEGDA 95/5 shows a similar characteristic of fracture with failure after a small deformation. The formation of necking cannot be seen for neat PLA and PLA/CPEGDA 95/5. On the contrary, with incorporation of CPEGDA at more contents (PLA/CPEGDA 90/10 and 85/15), the blend samples show distinct yielding and stable necking development. The elongations at break for PLA/CPEGDA 90/10 and 85/15 reach around 160% and 140%, respectively. With further increase of CPEGDA contents to 20 and 25%, the fracture of blends happens earlier during tensile deformation with the elongations at break dropping to 31% and 26% for PLA/CPEGDA 80/20 and 75/25, respectively.

The changes of tensile toughness, notched Izod impact strength, yield strength, and tensile modulus as functions of

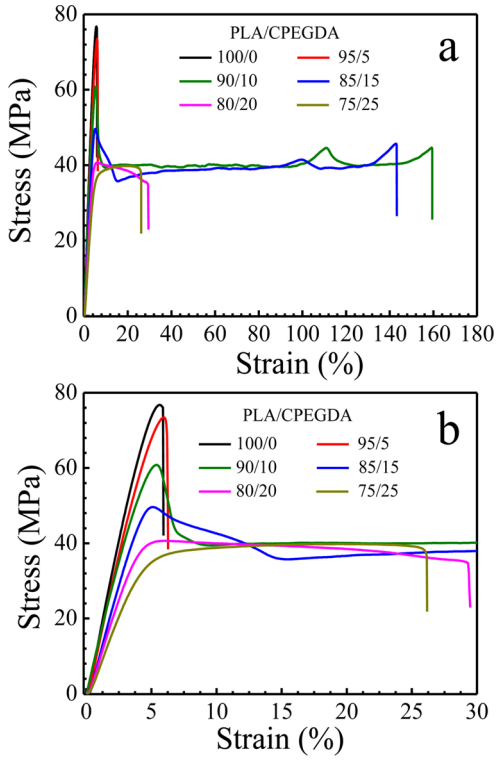

Figure 8. Typical nominal stress−strain curves for neat PLA and PLA/CPEGDA blends with different mass ratios in (a) a full strain range and (b) a low strain range.

CPEGDA content for the blends are collectively shown in Figure 9. The comparative changing trends in tensile toughness and notched Izod impact strength with increasing CPEGDA content shown in Figure 9a illustrate that the enhancement of toughness is achieved by incorporating PEGDA in the PLA matrix via melt blending process, for example, PLA/CPEGDA 85/15 exhibits remarkably improvements in both tensile toughness and notched Izod impact strength, with the tensile toughness (55 ± 6 MJ/m^3) and notched Izod impact strength (50 ± 8 MJ/m^2) of 20 and 26 times higher than that of neat PLA (tensile toughness 2.7 ± 0.1 MJ/m^3; notched Izod impact strength 1.9 ± 0.4 MJ/m^2), respectively. Similar to other toughness-modified PLA blends, the incorporation of CPEGDA possesses negative effect to the rigid strength of PLA materials. The tensile modulus and yield strength of the blends suffer reductions with increasing CPEGDA content. As compared with neat PLA, the tensile modulus for PLA/CPEGDA 85/15 decreases to 1.3 GPa (1.8 GPa for neat PLA) and yield strength decreases to 49 MPa (77 MPa for neat PLA).

Phase Morphologies of the Blends by TEM. It is well-known that the phase morphologies, the sizes of dispersed phase domains and distances between dispersed phase domains are crucial factors that determine the mechanical properties of polymer blends. The results from the phase contrast optical microscope observation and DSC measurements have indicated immiscibility between PLA and CPEGDA. Further phase morphological observation by using TEM was performed for PLA/CPEGDA blends. Figure 10 shows the TEM micrographs for neat PLA and PLA/CPEGDA blends with different mass ratios. CPEGDA particles with irregular shapes are dispersed in PLA matrix as the minor phase domains, and the phase boundaries of the particles are coarse and devoid of sharp demarcation, indicating the formation of sufficient interfacial

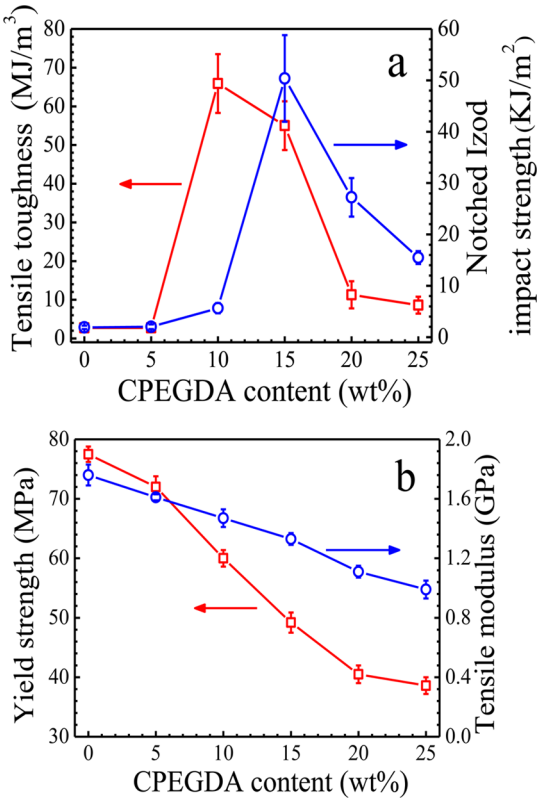

Figure 9. Changes of (a) tensile toughness and notched Izod impact strength and (b) yield strength and tensile modulus as functions of CPEGDA content for neat PLA and PLA/CPEGDA blends with different mass ratios. Note that the tensile toughness values are determined by the areas under the nominal stress–strain curves.

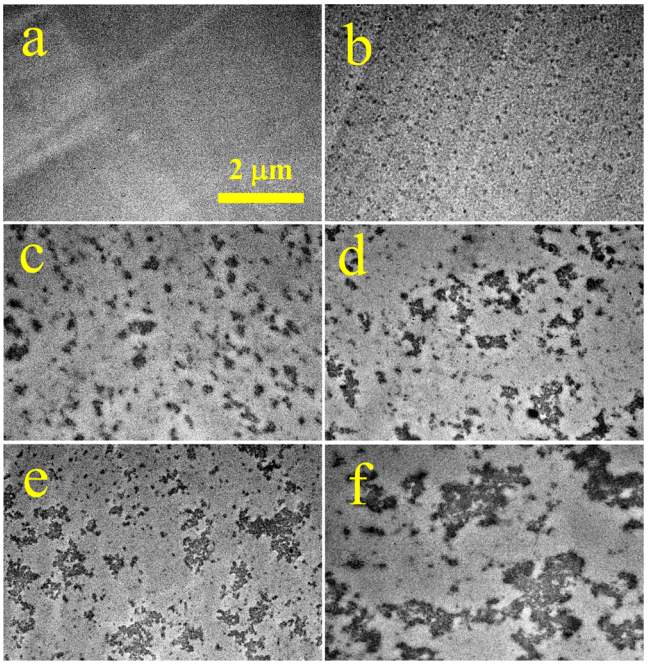

Figure 10. TEM micrographs of (a) neat PLA and PLA/CPEGDA blends with different mass ratios of (b) 95/5, (c) 90/10, (d) 85/15, (e) 80/20, and (f) 75/25. The yellow scale bar in panel a represents 2 μm and is applied to all other micrographs.

areas. In PLA/CPEGDA 95/5, small and uniform particles are clearly seen (Figure 10b). With increasing CPEGDA content, the coalescence of the dispersed phase domains takes place, leading to increased particle sizes and size distributions (Figures 10c–f). The average particle sizes and size distributions of the dispersed phase domains are measured and summarized in Table 2. It is found that the mass-average particle diameter, d_m increases from 0.072 to 1.20 μm and the size polydispersity, d_m/d_n increases from 1.0 to 2.0 with increasing CPEGDA content from 5 to 25 wt % for PLA/CPEGDA blends.

Table 2. Phase Morphological Parameters for PLA/CPEGDA Blends with Different Mass Ratios

sample code	d_n (μm)	d_m (μm)	d_m/d_n	T (μm)
PLA/CPEGDA 95/5	0.069	0.072	1.0	1.60
PLA/CPEGDA 90/10	0.27	0.31	1.2	0.28
PLA/CPEGDA 85/15	0.24	0.35	1.5	0.27
PLA/CPEGDA 80/20	0.36	0.63	1.8	0.41
PLA/CPEGDA 75/25	0.60	1.20	2.0	0.82

In this work, the dispersed CPEGDA phase domains are in situ formed in the continuous PLA matrix by reactive blending as schematically illustrated in Scheme 3. The PEGDA monomer is miscible with PLA matrix in the initial stage of mixing (stage I), and then in the reactive melt blending process (stage II), CPEGDA particles are formed in PLA matrix by the thermally initiated polymerization of PEGDA monomer. The solubility parameter of PEGDA monomer changes when PEGDA polymerizes into cross-linked particles, leading to the phase separated morphology with a fine dispersion state (stage III). The sufficient interfacial adhesion (formation of interfacial layers) is achieved by the compatibilization effect of the dangling PEG chains and interfacial transesterification between cross-linked PEGDA phase domains and PLA matrix. With increasing PEGDA content in the blends, the acrylate groups are prone to polymerize and form cross-linked PEGDA due to the higher reactivity than transesterification, leading to coalescence of CPEGDA. As a result, the CPEGDA particle sizes and size distributions in the blends increase with increasing CPEGDA content.

Toughening Mechanism. Toughness implies energy absorption in a deformation process of polymer materials and the improvement in toughness can be explained by a number of mechanisms, including crazing and shear yielding. The toughening effects of CPEGDA particles in the blends are analyzed from the following two aspects.

In the first aspect, the tensile deformation behavior of PLA/CPEGDA 85/15 with optimum mechanical properties is analyzed to reveal the possible toughening mechanism. When this sample was subjected to tensile deformation, stress-whitening was observed in the initial state of deformation due to the light scattering by numerous tiny crazes. The fine dispersed CPEGDA particles can provide control over nucleation and growth of crazes and increase craze plasticity, leading to decrease in brittleness. Notably, this blend shows a combination of strain-softening and cold-drawing in the stress–strain curve beyond the yield point (Figure 8b). In this region, there exists a competition between craze formation and shear yielding. There is a drop in stress with increasing strain beyond the yield point of 5% strain. After the strain of 15% only cold-drawing dominates with constant stress. This phenomenon suggests an occurrence of large energy dissipation. Similar

Scheme 3. Schematic Illustration of Formation of the Dispersed CPEGDA Phase Domains in PLA Matrix during the Reactive Melt Blending Process

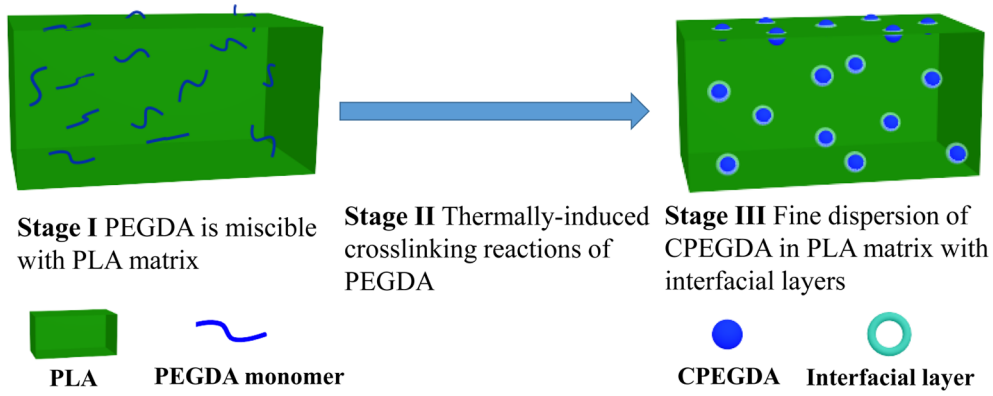

behavior in uniaxial tensile drawing was reported for toughened PLA-graft copolymers[13] and PLA/hyper-branched polymer (HBP) blends.[30]

The fracture surfaces of the tensile test sample bars were examined by SEM and the results are shown in Figure 11. Neat

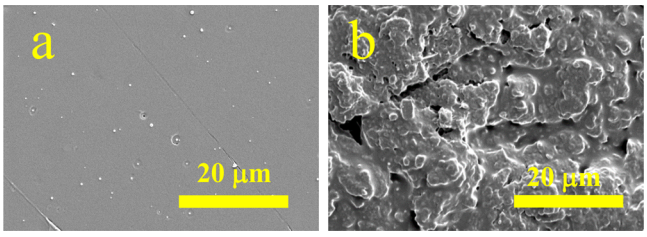

Figure 11. SEM micrographs of (a) neat PLA and (b) PLA/CPEGDA blend with mass ratio of 85/15.

PLA shows a smooth and featureless fracture surface without much deformation, indicating a typical brittle fracture behavior. The surface of PLA/CPEGDA 85/15 exhibits rugged feature with some voids, indicating that the PLA matrix experiences shear yielding, which could be induced by cavitation of the rubbery particles. Therefore, the fracture energy in the high strain region is mainly dissipated by shear yielding mechanism.

In the second aspect, the values of matrix ligament thickness (T) in the PLA/CPEGDA blends are estimated to explain the improvement of toughness. As first proposed by Wu,[63,64] there exists a minimum confinement length governing the onset of ductility of polymer blends. The confinement is usually characterized by a critical distance between neighboring dispersed particles known as the critical matrix ligament thickness. It is stated that if the average matrix ligament thickness is below the critical value, the blend could be tough, and if it is above the critical value, the blend could be brittle. Hillmyer et al. reported that there was a critical matrix ligament thickness for toughing PLA, which was approximately 1.0 μm.[65] In this work, the values of matrix ligament thickness in PLA/CPEGDA blends are measured and summarized in Table 2. Except for that of PLA/CPEGDA 95/5, the T values are smaller than the critical value of 1.0 μm, providing a good interpretation for the improved toughness of PLA/CPEGDA blends. The matrix ligament thickness decreases with increasing CPEGDA content and reaches the minimum value for PLA/CPEGDA 85/15, which shows the optimum tensile toughness and notched Izod impact strength. It should be mentioned that PLA/CPEGDA 90/10 demonstrates different deformation performance in tensile and impact tests, even though it has comparable matrix ligament thickness with PLA/CPEGDA 85/15. This disagreement in tensile and impact toughness is due to the different strain rates during fracture. However, their correlations with the microstructures of the blends still remain open for further investigation. The obvious increases in the matrix ligament thickness for the blends with 20 and 25 wt % contents of CPEGDA are caused by larger particle sizes and size distributions (Table 2), leading to deterioration of both tensile toughness and notched Izod impact strength.

On the whole, the improvement of toughness in PLA/CPEGDA blends is ascribed to the jointly contributions of crazing and shear yielding. They play important roles to dissipate deformation energy at different deformation strains: crazing dominates in the lower strain region and shear yielding becomes the main factor in the larger strain region.

CONCLUSIONS

In this work, supertough PLA materials consisting of PLA and cross-linked PEGDA (CPEGDA) were successfully prepared by in situ reactive melt blending of PLA and PEG-based diacrylate monomer (PEGDA) with no addition of any exogenous radical initiators. The polymerization of acylate groups in PEGDA occurred in PLA matrix and the resulted CPEGDA particles could act as efficient toughening modifier, which brought out supertoughness to the PLA materials. The PLA materials show a phase separated morphology containing dispersed CPEGDA particles and PLA matrix. High values of complex viscosity and storage modulus were achieved by incorporation of CPEGDA in the blends and the rheological percolation reached at the CPEGDA content of 15 wt %. The crystallinity values obtained from the specimens for mechanical property tests indicated that PLA in the blends was in the amorphous state and the introduction of CPEGDA had little effect on the crystallization kinetics of PLA. Both tensile toughness and notched Izod impact strength were significantly increased for the PLA materials and the optimized mechanical properties were achieved for the blend containing CPEGDA of 15 wt %. The significant improvement in toughness could be attributed to the fine dispersion state of CPEGDA particles in PLA matrix with mass-average particle diameter of 0.35 μm and size polydispersity of 1.5. The toughening mechanisms were analyzed through three aspects, including observations of stress-whitening and the fracture surface, and measurement of matrix ligament thickness. These results reveal that the

improvements in toughness for PLA/CPEGDA blends are achieved according to the mechanisms of crazing and shear yielding at different strain regions, respectively.

■ ASSOCIATED CONTENT

Supporting Information

Changes of torque as functions of mixing time during reactive blending process, photos of PLA/PEGDA blend sheets prepared by solution casting and melt blending methods, and DSC heat flow curves of PLA/PEG blends in Figures S1−S3, summary of mechanical properties for neat PLA and PLA/CPEGDA blends in Table S1, and the steps to calculate the matrix ligament thickness in Note S1. This material is available free of charge via the Internet at http://pubs.acs.org/.

■ AUTHOR INFORMATION

Corresponding Authors

*E-mail: zgwang2@ustc.edu.cn.

*Tel.: +86 0551-63607703. Fax: +86 0551-63607703. E-mail: dingys@hfut.edu.cn.

Notes

The authors declare no competing financial interest.

■ ACKNOWLEDGMENTS

Z.G.W. acknowledges the financial support from the National Science Foundation of China with Grant No. 21174139 and National Basic Research Program of China with Grant No. 2012CB025901. Y.S.D. acknowledges the financial support from the National Science Foundation of China with Grant No. 50973025 and 51373045. Dr. Sheng Cheng at Hefei University of Technology is acknowledged for assistance with the TEM observation.

■ REFERENCES

(1) Drumright, R. E.; Gruber, P. R.; Henton, D. E. Polylactic Acid Technology. *Adv. Mater.* **2000**, *12*, 1841−1846.

(2) Jamshidian, M.; Tehrany, E. A.; Imran, M.; Jacquot, M.; Desobry, S. Poly-Lactic Acid: Production, Applications, Nanocomposites, and Release Studies. *Compr. Rev. Food Sci. Food Saf.* **2010**, *9*, 552−571.

(3) Gross, R. A.; Kalra, B. Biodegradable Polymers for the Environment. *Science* **2002**, *297*, 803−807.

(4) Yu, L.; Dean, K.; Li, L. Polymer Blends and Composites from Renewable Resources. *Prog. Polym. Sci.* **2006**, *31*, 576−602.

(5) Lim, L. T.; Auras, R.; Rubino, M. Processing Technologies for Poly(Lactic Acid). *Prog. Polym. Sci.* **2008**, *33*, 820−852.

(6) Tonelli, A. E.; Flory, P. J. The Configurational Statistics of Random Poly(Lactic Acid) Chains. I. Experimental Results. *Macromolecules* **1969**, *2*, 225−227.

(7) Grijpma, D.; Penning, J.; Pennings, A. Chain Entanglement, Mechanical Properties and Drawability of Poly(Lactide). *Colloid Polym. Sci.* **1994**, *272*, 1068−1081.

(8) Joziasse, C. A.; Veenstra, H.; Grijpma, D. W.; Pennings, A. J. On the Chain Stiffness of Poly(Lactide) S. *Macromol. Chem. Phys.* **1996**, *197*, 2219−2229.

(9) Liu, H. Z.; Zhang, J. W. Research Progress in Toughening Modification of Poly(Lactic Acid). *J. Polym. Sci., Part B: Polym. Phys.* **2011**, *49*, 1051−1083.

(10) Bitinis, N.; Sanz, A.; Nogales, A.; Verdejo, R.; Lopez-Manchado, M. A.; Ezquerra, T. A. Deformation Mechanisms in Polylactic Acid/Natural Rubber/Organoclay Bionanocomposites as Revealed by Synchrotron X-Ray Scattering. *Soft Matter* **2012**, *8*, 8990−8997.

(11) Liu, H.; Chen, N.; Fujinami, S.; Louzguine-Luzgin, D.; Nakajima, K.; Nishi, T. Quantitative Nanomechanical Investigation on Deformation of Poly(Lactic Acid). *Macromolecules* **2012**, *45*, 8770−8779.

(12) Jing, F.; Hillmyer, M. A. A Bifunctional Monomer Derived from Lactide for Toughening Polylactide. *J. Am. Chem. Soc.* **2008**, *130*, 13826−13827.

(13) Theryo, G.; Jing, F.; Pitet, L. M.; Hillmyer, M. A. Tough Polylactide Graft Copolymers. *Macromolecules* **2010**, *43*, 7394−7397.

(14) Castillo, J. A.; Borchmann, D. E.; Cheng, A. Y.; Wang, Y.; Hu, C.; Garcia, A. J.; Weck, M. Well-Defined Poly(Lactic Acid)S Containing Poly(Ethylene Glycol) Side-Chains. *Macromolecules* **2012**, *45*, 62−69.

(15) Lee, I.; Panthani, T. R.; Bates, F. S. Sustainable Poly(Lactide-*b*-butadiene) Multiblock Copolymers with Enhanced Mechanical Properties. *Macromolecules* **2013**, *46*, 7387−7398.

(16) Bitinis, N.; Verdejo, R.; Bras, J.; Fortunati, E.; Kenny, J. M.; Torre, L.; Lopez-Manchado, M. A. Poly(Lactic Acid)/Natural Rubber/Cellulose Nanocrystal Bionanocomposites Part I. Processing and Morphology. *Carbohydr. Polym.* **2013**, *96*, 611−620.

(17) Bitinis, N.; Fortunati, E.; Verdejo, R.; Bras, J.; Kenny, J. M.; Torre, L.; Lopez-Manchado, M. A. Poly(Lactic Acid)/Natural Rubber/Cellulose Nanocrystal Bionanocomposites. Part II: Properties Evaluation. *Carbohydr. Polym.* **2013**, *96*, 621−627.

(18) Chang, K.; Robertson, M. L.; Hillmyer, M. A. Phase Inversion in Polylactide/Soybean Oil Blends Compatibilized by Poly(Isoprene-*b*-Lactide) Block Copolymers. *ACS Appl. Mater. Interfaces* **2009**, *1*, 2390−2399.

(19) Robertson, M. L.; Paxton, J. M.; Hillmyer, M. A. Tough Blends of Polylactide and Castor Oil. *ACS Appl. Mater. Interfaces* **2011**, *3*, 3402−3410.

(20) Scott, C. E.; Macosko, C. W. Morphology Development During Reactive and Non-Reactive Blending of an Ethylene−Propylene Rubber with Two Thermoplastic Matrices. *Polymer* **1994**, *35*, 5422−5433.

(21) Sailer, C.; Handge, U. Reactive Blending of Polyamide 6 and Styrene− Acrylonitrile Copolymer: Influence of Blend Composition and Compatibilizer Concentration on Morphology and Rheology. *Macromolecules* **2008**, *41*, 4258−4267.

(22) Pernot, H.; Baumert, M.; Court, F.; Leibler, L. Design and Properties of Co-Continuous Nanostructured Polymers by Reactive Blending. *Nat. Mater.* **2002**, *1*, 54−58.

(23) Xu, H. J.; Zhang, Y. Q.; Yang, J. J.; Ye, L.; Wu, Q. H.; Qu, B. J.; Wang, Q.; Wang, Z. G. Simultaneous Enhancements of Toughness and Tensile Strength for Thermoplastic/Elastomer Blends through Interfacial Photocrosslinking with Uv Radiation. *Polym. Chem.* **2013**, *4*, 3028−3038.

(24) Jiang, W.; Liu, C. H.; Wang, Z. G.; An, L. J.; Liang, H. J.; Jiang, B. Z.; Wang, X. H.; Zhang, H. X. Brittle-Tough Transition in PP/EPDM Blends: Effects of Interparticle Distance and Temperature. *Polymer* **1998**, *39*, 3285−3288.

(25) Oyama, H. T. Super-Tough Poly(Lactic Acid) Materials: Reactive Blending with Ethylene Copolymer. *Polymer* **2009**, *50*, 747−751.

(26) Liu, H. Z.; Chen, F.; Liu, B.; Estep, G.; Zhang, J. W. Super Toughened Poly(Lactic Acid) Ternary Blends by Simultaneous Dynamic Vulcanization and Interfacial Compatibilization. *Macromolecules* **2010**, *43*, 6058−6066.

(27) Liu, H. Z.; Song, W. J.; Chen, F.; Guo, L.; Zhang, J. W. Interaction of Microstructure and Interfacial Adhesion on Impact Performance of Polylactide Ternary Blends. *Macromolecules* **2011**, *44*, 1513−1522.

(28) Liu, H. Z.; Guo, L.; Guo, X. J.; Zhang, J. W. Effects of Reactive Blending Temperature on Impact Toughness of Poly(Lactic Acid) Ternary Blends. *Polymer* **2012**, *53*, 272−276.

(29) Liu, H. Z.; Guo, X. J.; Song, W. J.; Zhang, J. W. Effects of Metal Ion Type on Ionomer-Assisted Reactive Toughening of Poly(Lactic Acid). *Ind. Eng. Chem. Res.* **2013**, *52*, 4787−4793.

(30) Bhardwaj, R.; Mohanty, A. K. Modification of Brittle Polylactide by Novel Hyperbranched Polymer-Based Nanostructures. *Biomacromolecules* **2007**, *8*, 2476−2484.

(31) Xiong, Z.; Yang, Y.; Feng, J.; Zhang, X.; Zhang, C.; Tang, Z.; Zhu, J. Preparation and Characterization of Poly(Lactic Acid)/Starch

Composites Toughened with Epoxidized Soybean Oil. *Carbohydr. Polym.* **2013**, *92*, 810−816.
(32) Xiong, Z.; Zhang, L.; Ma, S.; Yang, Y.; Zhang, C.; Tang, Z.; Zhu, J. Effect of Castor Oil Enrichment Layer Produced by Reaction on the Properties of PLA/HDI-G-Starch Blends. *Carbohydr. Polym.* **2013**, *94*, 235−243.
(33) Wang, L.; Ma, W.; Gross, R.; McCarthy, S. Reactive Compatibilization of Biodegradable Blends of Poly(Lactic Acid) and Poly(ε-Caprolactone). *Polym. Degrad. Stab.* **1998**, *59*, 161−168.
(34) Bai, H.; Xiu, H.; Gao, J.; Deng, H.; Zhang, Q.; Yang, M.; Fu, Q. Tailoring Impact Toughness of Poly(L-Lactide)/Poly(Epsilon-Caprolactone) Blends by Controlling Crystallization of PLLA Matrix. *ACS Appl. Mater. Interfaces* **2012**, *4*, 897−905.
(35) Xu, Z. H.; Zhang, Y. Q.; Wang, Z. G.; Sun, N.; Li, H. Enhancement of Electrical Conductivity by Changing Phase Morphology for Composites Consisting of Polylactide and Poly (ε-Caprolactone) Filled with Acid-Oxidized Multiwalled Carbon Nanotubes. *ACS Appl. Mater. Interfaces* **2011**, *3*, 4858−4864.
(36) Ojijo, V.; Sinha Ray, S.; Sadiku, R. Role of Specific Interfacial Area in Controlling Properties of Immiscible Blends of Biodegradable Polylactide and Poly[(Butylene Succinate)-*co*-Adipate]. *ACS Appl. Mater. Interfaces* **2012**, *4*, 6690−701.
(37) Ojijo, V.; Sinha Ray, S.; Sadiku, R. Toughening of Biodegradable Polylactide/Poly(Butylene Succinate-*co*-Adipate) Blends Via in Situ Reactive Compatibilization. *ACS Appl. Mater. Interfaces* **2013**, *5*, 4266−76.
(38) Kang, H.; Qiao, B.; Wang, R.; Wang, Z.; Zhang, L.; Ma, J.; Coates, P. Employing a Novel Bioelastomer to Toughen Polylactide. *Polymer* **2013**, *54*, 2450−2458.
(39) Gramlich, W. M.; Robertson, M. L.; Hillmyer, M. A. Reactive Compatibilization of Poly(L-Lactide) and Conjugated Soybean Oil. *Macromolecules* **2010**, *43*, 2313−2321.
(40) Xu, Y. Q.; Qu, J. P. Mechanical and Rheological Properties of Epoxidized Soybean Oil Plasticized Poly(Lactic Acid). *J. Appl. Polym. Sci.* **2009**, *112*, 3185−3191.
(41) Harris, J. M. *Poly(Ethylene Glycol) Chemistry: Biotechnical and Biomedical Applications*; Springer: New York, 1992.
(42) Hu, Y.; Rogunova, M.; Topolkaraev, V.; Hiltner, A.; Baer, E. Aging of Poly (Lactide)/Poly(Ethylene Glycol) Blends. Part 1. Poly(Lactide) with Low Stereoregularity. *Polymer* **2003**, *44*, 5701−5710.
(43) Lai, W. C.; Liau, W. B.; Lin, T. T. The Effect of End Groups of PEG on the Crystallization Behaviors of Binary Crystalline Polymer Blends PEG/PLLA. *Polymer* **2004**, *45*, 3073−3080.
(44) Hu, Y.; Hu, Y.; Topolkaraev, V.; Hiltner, A.; Baer, E. Aging of Poly (Lactide)/Poly(Ethylene Glycol) Blends. Part 2. Poly(Lactide) with High Stereoregularity. *Polymer* **2003**, *44*, 5711−5720.
(45) Zhang, Y. Q.; Xu, H. J.; Yang, J. J.; Chen, S. Y.; Ding, Y. S.; Wang, Z. G. Significantly Accelerated Spherulitic Growth Rates for Semicrystalline Polymers through the Layer-by-Layer Film Method. *J. Phys. Chem. C* **2013**, *117*, 5882−5893.
(46) Zhang, Y. Q.; Wang, Z. K.; Jiang, F.; Bai, J.; Wang, Z. G. Effect of Miscibility on Spherulitic Growth Rate for Double-Layer Polymer Films. *Soft Matter* **2013**, *9*, 5771−5778.
(47) Zhang, Y. Q.; Fang, H. G.; Wang, Z. K.; Tang, M.; Wang, Z. G. Disclosing the Formation of Ring-Banded Spherulites for Semicrystalline Polymers through the Double-Layer Film Method. *CrystEngComm* **2014**, *16*, 1026−1037.
(48) Hassouna, F.; Raquez, J.-M.; Addiego, F.; Dubois, P.; Toniazzo, V.; Ruch, D. New Approach on the Development of Plasticized Polylactide: Grafting of Poly(Ethylene Glycol) Via Reactive Extrusion. *Eur. Polym. J.* **2011**, *47*, 2134−2144.
(49) Park, B. S.; Song, J. C.; Park, D. H.; Yoon, K. B. PLA/Chain-Extended PEG Blends with Improved Ductility. *J. Appl. Polym. Sci.* **2012**, *123*, 2360−2367.
(50) Liu, G. C.; He, Y. S.; Zeng, J. B.; Xu, Y.; Wang, Y. Z. In Situ Formed Crosslinked Polyurethane Toughened Polylactide. *Polym. Chem.* **2014**, *5*, 2530−2540.
(51) Choi, K. M.; Choi, M. C.; Han, D. H.; Park, T. S.; Ha, C. S. Plasticization of Poly(Lactic Acid) through Chemical Grafting of Poly(Ethylene Glycol) Via in Situ Reactive Blending. *Eur. Polym. J.* **2013**, *49*, 2356−2364.
(52) Garlotta, D. A Literature Review of Poly(Lactic Acid). *J. Polym. Environ.* **2001**, *9*, 63−84.
(53) Liu, Z. H.; Zhang, X. D.; Zhu, X. G.; Li, R. K.Y.; Qi, Z. N.; Wang, F. S.; Choy, C. L. Effect of Morphology on the Brittle Ductile Transition of Polymer Blends: 2. Analysis on Poly(Vinyl Chloride)/Nitrile Rubber Blends. *Polymer* **1998**, *39*, 5019−5025.
(54) Lin, H.; Kai, T.; Freeman, B. D.; Kalakkunnath, S.; Kalika, D. S. The Effect of Cross-Linking on Gas Permeability in Cross-Linked Poly(Ethylene Glycol Diacrylate). *Macromolecules* **2005**, *38*, 8381−8393.
(55) Lin, H.; Freeman, B. D. Gas Permeation and Diffusion in Cross-Linked Poly(Ethylene Glycol Diacrylate). *Macromolecules* **2006**, *39*, 3568−3580.
(56) Lee, S. H.; Lee, W. G.; Chung, B. G.; Park, J. H.; Khademhosseini, A. Rapid Formation of Acrylated Microstructures by Microwave-Induced Thermal Crosslinking. *Macromol. Rapid Commun.* **2009**, *30*, 1382−1386.
(57) Liu, C.; Lin, S.; Zhou, C.; Yu, W. Influence of Catalyst on Transesterification between Poly(Lactic Acid) and Polycarbonate under Flow Field. *Polymer* **2013**, *54*, 310−319.
(58) Coltelli, M.-B.; Toncelli, C.; Ciardelli, F.; Bronco, S. Compatible Blends of Biorelated Polyesters through Catalytic Transesterification in the Melt. *Polym. Degrad. Stab.* **2011**, *96*, 982−990.
(59) Winter, H. H.; Chambon, F. Analysis of Linear Viscoelasticity of a Crosslinking Polymer at the Gel Point. *J. Rheol.* **1986**, *30*, 367−382.
(60) Chambon, F.; Winter, H. H. Linear Viscoelasticity at the Gel Point of a Crosslinking PDMS with Imbalanced Stoichiometry. *J. Rheol.* **1987**, *31*, 683−697.
(61) Li, W. L.; Zhang, Y. Q.; Yang, J. J.; Zhang, J.; Niu, Y. H.; Wang, Z. G. Thermal Annealing Induced Enhancements of Electrical Conductivities and Mechanism for Multiwalled Carbon Nanotubes Filled Poly(Ethylene-*co*-hexene) Composites. *ACS Appl. Mater. Interfaces* **2012**, *4*, 6468−6478.
(62) Izuka, A.; Winter, H. H.; Hashimoto, T. Self-Similar Relaxation Behavior at the Gel Point of a Blend of a Cross-Linking Poly(ε-Caprolactone) Diol with a Poly(Styrene-*co*-Acrylonitrile). *Macromolecules* **1997**, *30*, 6158−6165.
(63) Wu, S. Phase Structure and Adhesion in Polymer Blends: A Criterion for Rubber Toughening. *Polymer* **1985**, *26*, 1855−1863.
(64) Wu, S. A Generalized Criterion for Rubber Toughening: The Critical Matrix Ligament Thickness. *J. Appl. Polym. Sci.* **1988**, *35*, 549−561.
(65) Anderson, K. S.; Lim, S. H.; Hillmyer, M. A. Toughening of Polylactide by Melt Blending with Linear Low-Density Polyethylene. *J. Appl. Polym. Sci.* **2003**, *89*, 3757−3768.